

# Base-Sequence Dependence of Emission Lifetimes for DNA Oligomers and Duplexes Covalently Labeled with Pyrene: Relative Electron-Transfer Quenching Efficiencies of A, G, C, and T Nucleosides toward Pyrene\*

Muthiah Manoharan and Kathleen L. Tivel

Isis Pharmaceuticals, Inc., 2280 Faraday Avenue, Carlsbad, California 92008

Min Zhao, Kambiz Nafisi, and Thomas L. Netzel\*

Department of Chemistry, Georgia State University, Atlanta, Georgia 30303

Received: June 29, 1995; In Final Form: August 30, 1995<sup>⊗</sup>

This paper reports both continuous and time-resolved spectroscopic studies of the emission properties of photoexcited pyrene labels covalently attached to uridine nucleosides and oligonucleotides. For all nucleic acid systems, uridine is substituted with pyrene at the 2'-oxygen position, 2'-O-[hexyl-N-(1-pyrenepropyl-carbonyl)amino]uridine, U(12)\*. Three types of nucleic acid systems are investigated: the 5'-OH (1) and the 5'-ODMT (2) substituted U(12)\*-nucleosides; four pentameric oligonucleotides, X<sub>2</sub>U(12)\*X<sub>2</sub>, where X is 2'-deoxyadenosine (A), 2'-deoxyguanosine (G), 2'-deoxythymidine (T), or 2'-deoxycytidine (C); and four duplexes with 18 base pairs each containing one strand with a central U(12)\* label. The central U(12)\* label in the duplexes has the following flanking base-sequences, 5'...AX<sub>2</sub>U(12)\*X<sub>2</sub>A...3', where X is A, G, T, or C. The 400-nm region emission kinetics for the four U(12)\*-labeled pentamers establish the following order of pyrene\*-quenching reactivities by flanking DNA bases: A < G < T < C. This ordering of reactivities is generally consistent with expected reactivities based on estimates of the free energies of pyrene\* quenching by electron transfer, ΔG°(ET), to or from flanking DNA bases. Emission spectra and lifetimes in the 495-nm region for both U(12)\*-labeled pentamers and duplexes provide direct evidence for the formation and decay of the pyrene<sup>+</sup>/U(12)<sup>-</sup> charge-transfer (CT) product. In general ca. 20% of the amplitude of the CT emission decays in the 1–7 ns time range and 70–80% of its amplitude decays in ≤0.2 ns. The C<sub>2</sub>U(12)\*C<sub>2</sub> pentamer has uniquely short π,π\* emission decay with its longest emission-lifetime component lasting only 5.6 ns and its average emission lifetime ≤0.6 ns. (In contrast the longest π,π\* emission components for pyrene butanoic acid (PBA) and U(12)\*OH (1) in methanol last, respectively, 231 and 37 ns.) Finally, the longest π,π\* emission lifetimes of U(12)\*-labeled DNA duplexes exceed those of the corresponding pentamers. A measure of duplex-induced restricted access of pyrene\* to base-paired nucleosides in double-strand (ds) versus single-strand (ss) DNA can be obtained by noting that the average π,π\* emission lifetimes (for greater than 1 ns components) lengthen 3-fold on going from the T<sub>2</sub>U(12)\*T<sub>2</sub> pentamer to the corresponding ...AT<sub>2</sub>U(12)\*T<sub>2</sub>A... duplex and 9-fold on going from the C<sub>2</sub>U(12)\*C<sub>2</sub> pentamer to the ...AC<sub>2</sub>U(12)\*C<sub>2</sub>A... duplex.

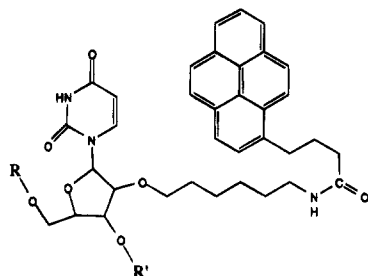
## Introduction

Pyrene is a stable molecule with a reasonably long fluorescence lifetime (ca. 200–400 ns) depending upon the type of substitution and solvent. Its long emission lifetime is a consequence of the fact that absorption to its lowest-energy electronic excited state (S<sub>1</sub>) is dipole forbidden. Since it is conveniently derivatized at the 1-position, it has often been employed as a fluorescent label especially in biological studies. Pyrene can also be reversibly oxidized and reduced in both its ground and lowest-energy excited states. Recently its photo-physics has been extensively studied as a carcinogenic and mutagenic benzo[a]pyrenediol epoxide (BPDE) derivative bound to the exocyclic amino group of guanosine in native DNA (BPDE-N<sup>2</sup>-G).<sup>1–8</sup> In polar organic solvents G quenches the emission of photoexcited BPDE and yields pyrenyl radical anions. However, in the same solvents, the covalent adduct BPDE-N<sup>2</sup>-G does not show radical products on the greater than 10 ns time scale, but it does show enhanced triplet formation most likely due to intramolecular electron-transfer (ET) excited-state quenching followed by rapid back ET.<sup>1</sup> A recent study

of BPDE-N<sup>2</sup>-G by Geacintov et al.<sup>9</sup> is the first to provide unambiguous evidence of ET between photoexcited pyrene (pyrene\*) and a covalently attached nucleic acid base. In this work the benzo[a]pyrene group is reduced, and G is oxidized. Complementing this finding, a recent report by Netzel et al.<sup>10</sup> describes observation of pyrene-to-nucleoside charge-transfer emission from 5-(1-pyrenyl)-U in methanol (MeOH). These authors also report transient absorbance detection of the pyrene<sup>+</sup>/U<sup>-</sup> CT photoproduct in MeOH in ≤30 ps for the 5-(1-carboxypyrenyl)-U nucleoside, where U is 2'-deoxyuridine. The above studies firmly establish the ET nature of pyrene\* emission quenching by G and U nucleosides.<sup>1,9,10</sup>

However, in general it is possible for other processes to be important in the excited-state deactivation of pyrene\* by nucleic acid bases. To gain insight into broader aspects of such quenching processes, six 2'-deoxynucleosides were added individually to solutions of a photoexcited tetrahydroxytetrahydrobenzo[a]pyrene (BPT) analogue of BPDE and their static and dynamic quenching properties were measured. G, T, C, and U were all found to be strong dynamic quenchers of pyrene\* emission, but their quenching rates were so close to the diffusion-controlled limit that there was no dependence of ET

<sup>⊗</sup> Abstract published in *Advance ACS Abstracts*, October 15, 1995.



U(12)\*OH (1): R=H, R'=H  
 U(12)\*ODMT (2): R=dimethoxytrityl (DMT), R'=H  
 U(12)\*Phos (5): R=DMT,  
 R'=(2-cyanoethyl)-N,N-diisopropylaminophosphoryl  
 U(12)\*-oligomer: R=R'=phosphodiester link

**Figure 1.** Structural drawing of three pyrene-labeled uridine nucleosides, 1, 2, and 5, and of a pyrene-labeled uridine positioned at an internal substitution site, U(12)\*, in polynucleotide strand.

quenching rate upon the free energy ( $\Delta G^\circ$ ) for the reaction as would be expected if ET quenching were occurring.<sup>11–17</sup> In contrast, A and 2'-deoxyinosine were weak dynamic quenchers of pyrene\* emission. This latter result agrees with  $\Delta G^\circ$  estimates for these reactions as being less favorable than for the more reactive nucleosides.<sup>3,18–20</sup> Importantly, a recent nanosecond time scale transient absorbance study has shown that BPT<sup>+</sup> radical cations are formed with very small quantum yields when pyrene\* is quenched in 0.1 M aqueous C and T solutions.<sup>21</sup>

A number of studies have involved pyrene linked covalently to oligodeoxyribonucleotides and to oligoribonucleotides.<sup>22–29</sup> In general these studies have found that the amount of pyrene emission from the linked assemblies is very sensitive to the environment surrounding the pyrene label. One such study has concluded that 5'-linked pyrene labels are ideal for probing the binding and dynamics of RNA substrates.<sup>29</sup> A frequent finding in these studies is that the pyrene-labeled duplexes emit more strongly than do the corresponding labeled oligomers. One interesting study constructed a tripartite duplex with short 3' and 5' end-labeled oligomers, both complexed to a common 30-nucleotide-long complementary strand such that the two pyrene labels could contact each other in the middle of the duplex. However, pyrene–excimer emission was not seen.<sup>27</sup> In contrast pyrene–excimer emission has been observed in DNA duplexes with multiple covalent adducts of BPDE.<sup>5,6,30,31</sup>

Despite a significant number of studies involving the quenching of pyrene\* emission by nucleic acid bases, nucleosides, and nucleotides, a clear picture of relative reactivity of the different nucleic acids has not emerged.<sup>1–4,30–38</sup> Similarly, a number of oligomers and duplexes have been constructed with covalently attached pyrene labels, yet little systematic work has been done comparing how flanking bases affect the emission properties of these pyrene labels.<sup>2,22–27,29,30,39,40</sup> Finally, a number of labeling studies relied solely on continuous emission measurements and did not time-resolve the pyrene label's emission kinetics.

In this paper, we examine with both continuous and time-resolved spectroscopies the emission properties of pyrene labels covalently attached to three types of nucleic acid systems. The first is a simple ribonucleoside consisting of uridine joined at the 2'-oxygen to a 1-pyrene propyl carbonyl label, U(12)\*OH (1) (see Figure 1). The second is a set of four pentameric oligonucleotides with a central U(12)\*-nucleotide flanked symmetrically by pairs of A, T, C, and G nucleotides, X<sub>2</sub>U(12)\*X<sub>2</sub>. The third system incorporates these symmetrical pentamers as central units in complementary duplexes each of which is 18 base pairs (bp) long. The other 13 nucleotides in

each strand are either A or T, added to produce duplexes with sufficiently high melting temperatures ( $T_m$ ) that ca. 99% of the oligomers would be double-stranded at room temperature.<sup>41,42</sup>

The goals of this work are 2-fold. First, we want to establish a clearer picture of the relative reactivities of the various DNA bases toward ET quenching of pyrene\* emission. Second, we want to establish a better understanding of the differences in ET quenching efficiencies of pyrene\* labels in DNA oligomers versus duplexes. This information will facilitate more rational design of pyrene-labeled oligonucleotide systems. For example, one will be better able to judge how to design either longer-lived or very much shorter-lived pyrene\* labels based on the type of nucleoside attachment site and DNA or RNA base sequence surrounding the label. Also, it may be possible to design systems in which there is enhanced differential emission between ss and ds conformations.<sup>29,40</sup> Finally, maximizing pyrene\*-label ET emission quenching could, at the same time, maximize the production of either oxidized or reduced nucleotide bases. Such specifically produced oligonucleotide ionizations could provide starting points for studies of electron motion in DNA oligomers and duplexes<sup>18,43–53</sup> and of the mechanisms of radiation damage in DNA and RNA.<sup>18,54–59</sup>

## Materials and Methods

**Preparation of 5'-O-(DMT)-2'-O-[hexyl-N-(1-pyrenepropylcarbonyl)amino]uridine (2).** 5'-O-(DMT)-2'-O-[hexyl(Ω-N-phthalimido)amino]uridine (3) was synthesized as part of an earlier study<sup>60</sup> from dibutylstanyleneuridine which was prepared according to the procedure of Wagner et al.<sup>61</sup> and alkylated with 6-bromohexylphthalimide at either the 2'- or 3'-oxygen positions. The resulting mixture of 2'- and 3'-alkylated products was treated with dimethoxytrityl (DMT) chloride to protect the 5'-oxygen, and the two isomers were separated by silica gel chromatography. The structure of 3 was confirmed at this time by <sup>13</sup>C and <sup>1</sup>H NMR.<sup>60</sup> 3 was refluxed with hydrazine in MeOH to yield the free amine 5'-O-(DMT)-2'-O-(hexylamino)uridine (4) as described by Manoharan et al.<sup>62</sup> 4 was condensed with pentafluorophenyl-1-pyrene butyrate to yield 2 in the same manner as described elsewhere for the condensation of eicosenoic acid with 4.<sup>62</sup> Elemental analysis of the product 2 gave satisfactory results, and UV/vis spectroscopy confirmed the presence of both uridiny and pyrenyl chromophores in 2 (see Figure 1 for a structural drawing).

**Preparation of 2'-O-[Hexyl-N-(1-pyrenepropylcarbonyl)amino]uridine (1).** Compound 2 was dissolved in dichloromethane, and aqueous 80% acetic acid was added to remove the DMT group. After 30 min the solution was evaporated to dryness, loaded onto a silica column, and eluted with 10% MeOH in dichloromethane to give 1 (see Figure 1 for a structural drawing). UV/vis spectroscopy confirmed the presence of both uridiny and pyrenyl chromophores in 1.

**Preparation of 5'-O-[DMT]-2'-O-[hexyl-N-(1-pyrenepropylcarbonyl)amino]uridine-3'-O-(2-cyanoethyl)-N,N-diisopropyl Phosphoramidite (5).** 2 was phosphitylated to yield the phosphoramidite 5 exactly as described elsewhere for other 2'-oxygen derivatized nucleosides with amide linkages between ribose and an attached label.<sup>62</sup> 5 (see Figure 1 for a structural drawing) was used as described below to synthesize all of the U(12)\*-containing oligomers and duplexes studied here.

**Structures of the Pyrene-Labeled Nucleosides, Phosphoramidite Reagent, and Synthetic Oligonucleotides.** Figure 1 presents the structures of three pyrene labeled nucleosides, U(12)\*OH (1), U(12)\*ODMT (2), and U(12)\*Phos (5). Compound 5 is the phosphoramidite reagent that was used by the automated DNA synthesizer to make the polynucleotides listed

**TABLE 1: Summary of DNA Oligonucleotides and HPLC Retention Times**

ID	DNA sequence	retention time (min) <sup>a</sup>
I	A <sub>2</sub> U(12)*A <sub>2</sub>	31.15
II	G <sub>2</sub> U(12)*G <sub>2</sub>	31.04
III	T <sub>2</sub> U(12)*T <sub>2</sub>	31.60
IV	C <sub>2</sub> U(12)*C <sub>2</sub>	30.94
V	TAT ATA AAU(12)* AAA TAA TTT	25.04
VI	TAT ATA GGU(12)* GGT AAA TTT	24.75
VII	TAT ATA TTU(12)* TTT AAA TTT	24.66
VIII	TAT ATA CCU(12)* CCA TAA TTT	25.44
IX	GAU(12)*CT	30.67
Vc	AAA TTA TTT ATT TAT ATA	18.56
Vlc	AAA TTT ACC ACC TAT ATA	18.27
VIIc	AAA TTT AAA AAA TAT ATA	18.13
VIIIc	AAA TTA TGG AGG TAT ATA	18.01

<sup>a</sup> Conditions: Waters Delta-Pak C<sub>18</sub>, 15  $\mu$ m, 300 Å column, 3.9  $\times$  300 mm. Gradient: 0–10 min, 5% CH<sub>3</sub>CN; 10–60 min, 5–80% CH<sub>3</sub>CN with 50 mM triethylammonium acetate pH = 7.0.

in Table 1. As shown in Figure 1, all of the U(12)\*-nucleosides in this study have pyrene joined at the 1-position via a 12-atom chain to the 2'-position of uridine. However, all other nucleotides in the synthetically prepared oligomers and duplexes in this study have 2'-deoxyribose units.

**Incorporation of 1 into Oligonucleotides.** Compound 5 (725 mg, 0.65 mmol) was dissolved in 5.5 mL of anhydrous acetonitrile and loaded onto an Applied Biosystems 380B DNA synthesizer to produce oligonucleotides. The amidite concentration was 0.12 M, and a coupling efficiency of 80–85% was observed. For the coupling step involving 5, the reaction time was extended to 15 min and this step was carried out twice. Except for this modification, standard protocols as specified by Applied Biosystems were followed. The oligomers were cleaved from the controlled pore glass (CPG) supports and deprotected under standard conditions using concentrated aqueous ammonia at 55 °C. The 5'-O-DMT-containing oligomers were then purified by reverse phase high-performance liquid chromatography (HPLC). Detritylation with aqueous 80% acetic acid and evaporation, followed by desalting in a Sephadex G-25 column gave oligonucleotides containing an internal pyrene-labeled uridine, U(12)\* (see Figure 1), as demonstrated by UV/vis absorbance spectra and emission spectra.

Table 1 lists the 5- and 18-membered oligonucleotides whose physical and photophysical properties are reported here. Also included in this table are identifying Roman numerals for these oligomers and their HPLC retention times. The pattern of retention times, which cluster for similar types of oligomers, and their reproducibility give confidence in the fidelity of the product output for the automatic DNA synthesizer used in this study, because the hydrophobicity of the pyrene label causes the pentamers to have the longest retention times (30–31 min) and the hydrophilicity of the unlabeled 18-mers causes them to have the shortest retention times (18–19 min). The balance between these competing attractions and repulsions with respect to water causes the pyrene labeled 18-mers to elute at intermediate retention times (24–25 min).

The 5-mer oligonucleotides I–IV are used in time-resolved emission studies to assess the relative reactivities of different flanking nucleosides with respect to quenching of the emission of a covalently attached pyrene\* label. The 18-mer oligonucleotides V–VIII, each of which contain an internal U(12)\* nucleotide, are mixed with equimolar amounts of the corresponding complementary oligonucleotides Vc–VIIIc to produce duplexes with a single internal U(12)\* nucleotide for time-resolved emission studies of pyrene\* quenching in duplexes.

Oligomer IX is used to verify by both proton and phosphorous NMR the purity and the correctness of the automatic synthesizer's product for an oligomer which is constructed from all five of the different kinds of phosphoramidite reagents used in this study. In the phosphorous NMR spectrum, four lines are observed between –0.4 and 0.0 ppm with respect to an H<sub>3</sub>PO<sub>4</sub> internal standard, as expected for the four inequivalent phosphodiester in pentamer IX. Additionally, one of these signals is 0.2 ppm downfield relative to the other three signals as expected for a pentamer with a single RNA nucleotide and three DNA nucleotides. In the proton NMR spectrum of IX, the five anomeric C1' protons and the two H5 protons of C and U(12)\* appear between 5.5 and 6.3 ppm and integrate to give an area equivalent to 7 protons. In addition, the other six carbon-attached protons on the bases of IX (three H6 protons on C, T, and U(12)\*, two H8 protons on A and G, and one H2 proton on A) and the nine aromatic protons on the pyrene label appear as a cluster of peaks between 7.4 and 8.5 ppm and integrate to give an area equivalent to 15 protons.

**Molar Extinction Coefficients, Fluorescence Spectra, and Quantum Yield Measurements.** Absorbance spectra were recorded on a Perkin-Elmer Lambda-6 spectrophotometer. Molar extinction coefficients ( $\epsilon_{\max}$ ) for pyrene labeled oligomers were based on a value of 43 100 M<sup>-1</sup> cm<sup>-1</sup> for pyrenebutanoic acid (PBA) in MeOH at 341 nm.<sup>63</sup> Two equal aliquots of a concentrated PBA solution in MeOH were diluted 10-fold with, respectively, MeOH and dimethyl sulfoxide (DMSO) to give the ratio of the PBA extinction coefficients in MeOH and DMSO. This yielded 44 200 M<sup>-1</sup> cm<sup>-1</sup> as the  $\epsilon_{\max}$  for PBA at 346 nm in DMSO. Subsequently, similarly diluted solutions of pyrene labeled oligomers were made in both phosphate buffer (described below) and DMSO. The above  $\epsilon_{\max}$  for PBA in DMSO was used to calculate the concentration of labeled oligomer in the two solutions and, therefore, the  $\epsilon_{\max}$  of each pyrene labeled oligomer in buffer. The logic of this procedure is based on the ability of DMSO to eliminate stacking interactions between nucleoside bases and the covalently attached pyrene label.<sup>28,29</sup> The  $\epsilon_{\max}$  values at 260 nm for unlabeled DNA oligomers which were used as complements for the labeled oligomers were calculated from literature values of  $\epsilon_{\max}$  for the constituent nucleotides.<sup>64</sup>

Fluorescence spectra were recorded on an SLM-8000C (SLM Aminco, Inc.) spectrofluorometer and corrected for the spectral response of the optical system. The correction factors were determined at Georgia State University by technical support personnel from SLM Aminco, Inc. using a standard lamp whose energy output was traceable to NIST calibrations. The excitation wavelength for emission spectra and quantum yield measurements was 341 nm. Also for relative emission quantum yield measurements, the excitation bandwidth was 1 nm, and the absorbances of the two samples being compared were made nearly identical at an absorbance value of ca. 0.1. Solutions for fluorescence measurements typically contained 1–4  $\mu$ M pyrene labeled sample in MeOH or in 7.5 mM monosodium phosphate buffer adjusted to pH 7.0 with 1.0 M NaCl and 1 mM Na<sub>2</sub>EDTA. The fluorescence quantum yield ( $\Phi_{\text{em}}$ ) for PBA in MeOH measured here was 0.065  $\pm$  0.02 relative to 9,10-diphenylanthracene in cyclohexane with  $\Phi_{\text{em}} = 1.00$ .<sup>65</sup> The fluorescence quantum yield for PBA in air-equilibrated phosphate buffer was measured to be 0.60 relative to 9,10-diphenylanthracene in cyclohexane. This result was also in good agreement with that determined by comparison to anthracene in cyclohexane with  $\Phi_{\text{em}} = 0.36$ .<sup>65</sup> The emission quantum yields of pyrene-labeled nucleosides, oligonucleotides, and duplexes were subsequently measured relative to PBA in either

MeOH or phosphate buffer solution as noted in the text. Appropriately oriented polarizers were used to eliminate the possible effects of nonisotropic fluorescence from the samples for both emission spectra and quantum yield measurements.<sup>66</sup> Also for samples with very weak emission an indirect emission quantum yield method was used for increased accuracy.<sup>67–70</sup> Samples used for emission spectra and quantum yield determinations were deaerated by bubbling with solvent saturated argon for 20–30 min while being magnetically stirred unless otherwise noted.

**Fluorescence Lifetime Measurements.** All fluorescence decays were recorded on a Tektronix SCD1000 transient digitizer ( $\leq 0.35$  ns rise time calculated from the bandwidth,  $\leq 120$  ps rise time for a step input 0.5 times the vertical range) and wavelength-resolved with a 0.1-m double-monochromator (Instruments SA, model DH10) in additive dispersion. 2-mm slits were used, producing an 8-nm bandpass. The 1200 grooves/mm holographic gratings were blazed at 450 nm. After passing through the monochromator, the emission was detected with a Hamamatsu 1564U microchannel plate (200 ps rise time). The excitation and emission beams were oriented at  $90^\circ$  with respect to each other with the Glan-Thompson emission polarizer set at  $54.7^\circ$  ("magic angle") with respect to the vertical excitation polarization to eliminate rotational diffusion artifacts in the emission lifetime measurements.<sup>66</sup> Emission for all lifetime measurements was excited at 355 nm with the third harmonic of an active-passive mode-locked  $\text{Nd}^{3+}$ :YAG laser manufactured by Continuum, Inc. Typically  $35\text{-}\mu\text{J}$  excitation pulses of ca. 25-ps duration were collimated into a 3-mm diameter beam and passed through a second Glan-Thompson polarizer before entering the sample cuvette. Photon Technology Incorporated software was modified by the manufacturer to process 1000 data points/decay curve and was used to deconvolute the instrument response from the emission decay to yield exponential lifetime fits to the emission decay data. Emission lifetime tests were carried out on commercial samples of anthracene (Aldrich, 99+%) and 1-aminoanthracene (Aldrich, 99+%) which were dissolved in cyclohexane and degassed in O-ring sealed optical cells with three FPT cycles on a vacuum line ( $2 \times 10^{-4}$  Torr). Recorded emission decays for these samples were fit with single exponential lifetimes of 5.1 and 22.5 ns, respectively, for anthracene and 1-aminoanthracene. These lifetimes agreed well with their respective literature values of 4.9 and 22.8 ns.<sup>65</sup> Additionally, all other pyrene labeled samples used for lifetime measurements were also vacuum degassed with three FPT cycles unless otherwise indicated.

The overall temporal resolution of the emission kinetics system is generally near 0.2 ns; however, in ideal circumstances it can be as good as ca. 50 ps after deconvolution. A detailed description of the lifetime fitting procedure used here is presented in a recent paper by Netzel et al.<sup>10</sup> for nine sets of emission decays on four time scales (20, 50, 100, and 500 ns) and includes the following: the equations used; plots of residual differences between experimental emission decays and calculated multi-exponential curves; linear and logarithmic plots of emission decays, lamp decays and exponential curves; and specific  $\chi_r^2$  (the reduced chi-square statistic) values for the plotted exponential curves.

Values for  $\chi_r^2$  for emission lifetime fits generally ranged from ca. 1 to 8; lower  $\chi_r^2$  values were generally obtained at wavelengths near emission maxima. It is worth noting that considerable loss of emission intensity was suffered in these experiments so that wavelength-resolved kinetics data could be obtained. Additionally, the interest in probing weak CT-emissions in the ca. 500-nm region as well as intense  $\pi, \pi^*$

emissions in the ca. 400-nm region necessarily meant that larger  $\chi_r^2$  values were obtained in the red region.

In general, the accuracy to which a lifetime component can be determined is proportional to the relative emission area of that component. For that reason relative area data are presented with the lifetime values. On the other hand, relative emission amplitudes are proportional to the number of emitting species with the corresponding lifetime; thus these data are also given. The combination of finite detector response time and small relative emission areas (1–3%) for a number of the subnanosecond lifetime components presented in this work causes such values to be highly uncertain. Emission lifetime components  $\geq 1$  ns generally also have significant relative emission areas and are consequently much more reliable. However, whenever two emission lifetimes are less than a factor of two different for either bi- or triexponential decay processes, relative amplitude errors of  $\pm 20\%$  and lifetime errors of  $\pm 10\text{--}20\%$  are common.<sup>71</sup> Typical errors for emission lifetimes that can be fit with only a single exponential are 2–4% for lifetimes  $\leq 10$  ns and 1–2% for lifetimes greater than 10 ns.

Emission kinetics were analyzed with the following criteria in mind: (1) reproducibility of a given measurement, (2) continuity of the variation of lifetimes as emission wavelength was varied (a global analysis), and (3) consistency of lifetime components found by fitting data from several time ranges. In addition to these criteria, Ockham's razor was used to demand that a significant improvement in  $\chi_r^2$  be made before an additional lifetime component be added. Generally, this was at least a 0.5–1.0 lowering of  $\chi_r^2$ . We did, however, find many times that the number of required lifetimes was robust. That is, an attempt to add another lifetime just repeated a previous lifetime component or an attempt to remove a lifetime component gave a very much larger  $\chi_r^2$  value.

The general fitting procedure began by insuring that each emission lifetime was recorded on a sufficiently coarse time scale so that its emission decayed into the noise (typically  $\pm 4\text{--}8$  counts compared to 10 000–12 000 counts in the signal's peak after background subtraction). These decay data were fit first, and their longest lifetime component was then used as a fixed lifetime in fits of data taken on finer time scales. The finer time scales allowed better resolution of the faster decay components. The finest time scale used in this work was 20 ns, corresponding to one time point every 20 ps. Each kinetics trace on each time scale recorded 1000 data points; all fits used all 1000 points; and all data curves which were fit were themselves the result of averaging 1000 photoexcitation events as well as 1000 background events and subtracting the latter from the former.

## Results

**Free Energies for Excited-State Electron-Transfer Quenching.** Electrochemical data on the oxidation and reduction of pyrene can be combined with similar redox data for nucleosides and the energy of the first excited  $\pi, \pi^*$  state of the pyrene label,  $E_{0,0}(\text{pyrene}^*)$ , to estimate free energies for excited-state electron-transfer quenching of pyrene\* within pyrene-labeled DNA molecules according to eq 1:<sup>72</sup>

$$\Delta G^\circ(\text{ET}) = e[E^\circ(\text{D}^+/\text{D}) - E^\circ(\text{A}/\text{A}^{\cdot-})] - E_{0,0}(\text{pyrene}^*) + w(r) \quad (1)$$

where  $E^\circ$  is a reduction potential, D is an electron donor, A is an electron acceptor, and  $w(r)$  is a coulombic interaction term between oxidized donor and reduced acceptor which represents free energy due to separating the ionic products at a distance  $r$

**TABLE 2: Nucleoside/Pyrene\* ET Quenching Free Energies<sup>a</sup>**

$\Delta G^\circ(\text{G}^+/\text{pyrene}^*), \text{eV}$	$\Delta G^\circ(\text{pyrene}^*/\text{C}^{\bullet-})$ and $\Delta G^\circ(\text{pyrene}^*/\text{T}^{\bullet-}),^b \text{eV}^2$
-0.33	-0.52

<sup>a</sup>  $E^\circ(\text{pyrene}^+/\text{pyrene}) = 1.28 \text{ V}$  (versus SCE);  $E^\circ(\text{pyrene}/\text{pyrene}^{\bullet-}) = -2.09 \text{ V}$  (versus SCE).<sup>1,83-85</sup> <sup>b</sup> It is likely that the reaction products should be written as  $\Delta G^\circ(\text{pyrene}^+/\text{C}(\text{H})^{\bullet-})$  and  $\Delta G^\circ(\text{pyrene}^+/\text{T}(\text{H})^{\bullet-})$ .

relative to each other,  $w(\infty) = 0.73,^{74}$  Generally in very polar media the magnitude of the coulombic term is less than ca. 0.1 eV and will be neglected here.<sup>3,11,73,75,76</sup> Depending on the redox properties of a given nucleoside, a pyrene label can be either reduced or oxidized when in its lowest energy  $\pi, \pi^*$  state.

The easiest nucleoside to oxidize is guanosine with a reduction potential for guanosine monophosphate cation ( $\text{GMP}^{\bullet+}/\text{GMP}$ ) of 0.83 V (versus a saturated calomel electrode (SCE)).<sup>18,19,77</sup> The easiest nucleosides to reduce are thymidine and cytidine with reduction potentials of -1.45 V (versus SCE).<sup>18,19,77</sup> However, because of the ready protonation of reduced cytosine in a DNA duplex by its base-paired partner guanosine, it is estimated that *in ds DNA* protonated reduced cytosine,  $\text{C}(\text{H})^{\bullet-}$ , is ca. 200 mV easier to form than is  $\text{T}^{\bullet-}$ .<sup>18,19</sup> Contrary to this opinion, bimolecular ET quenching of  $\text{BPT}^*$  by C and T is found to require a polar protic solvent, because it does not occur in the polar organic solvent DMSO.<sup>21</sup> This latter result implies that in water the products of the reductions of C and T are already the protonated reduced species, respectively,  $\text{C}(\text{H})^{\bullet-}$  and  $\text{T}(\text{H})^{\bullet-}$ . If this is true, the reduction potential of C will be the same *in water* and *in ds DNA*.<sup>78</sup>

Notably cytosine (Cy) can be protonated in three ways: (1) Carbon-6 (C6) is protonated irreversibly to form  $\text{Cy}(\text{C6})\text{H}^{\bullet+}$  with a rate constant of  $2.5 \times 10^3 \text{ s}^{-1}$ ,<sup>79</sup> this slow process is not important for excited state quenching. (2) Nitrogen-3 (N3) is reversibly protonated in ss and ds DNA to form  $\text{Cy}(\text{N3})\text{H}^{\bullet+}$ . (3) For ss DNA and the free base, the  $-\text{NH}_2$  group is reversibly protonated as result of specific cation association at N3 or low pH.<sup>80-82</sup> Only N3-protonation, however, is relevant to excited state electron transfer reactions in aqueous buffer at pH 7 with 1 M NaCl. Additionally, thymine<sup>•-</sup> can be protonated *irreversibly* at C6, but the rate constant is less than  $10^3 \text{ s}^{-1}$ .<sup>79</sup> The nucleoside redox values are combined in Table 2 with the 3.25 eV excited-state energy of pyrene butanoic acid (PBA) to yield estimates of the free energy of the most likely pyrene\*/DNA ET quenching processes.

For all three of the nucleosides in Table 2, ET quenching of pyrene\* is expected on the basis of  $\Delta G^\circ$  estimates to be exergonic. Also, similar considerations show that this is not expected to be the case for A. The actual rate of a given ET quenching event depends not only on  $\Delta G^\circ$  but also on electronic coupling and Franck-Condon factors.<sup>11,13,16,86-93</sup> However, for a series of related electron donor/acceptor (D/A) molecules held together by similar electrostatic and hydrophobic interactions, it is reasonable to assume that their ET quenching rates should be proportional to  $-\Delta G^\circ(\text{ET})$ . Whether or not possible ET quenching processes are in fact likely to be observed for pyrene-labeled ss and ds DNA cannot be estimated at present due to lack of information on their geometries, electronic couplings, and Franck-Condon factors (or reorganization energies).<sup>44,47,50,51,76,94-98</sup> A zero-order expectation, however, is that, to the extent the four nucleosides, A, G, T, and C, quench pyrene\* emission by means of ET, C, and T should react more rapidly than G. Also, A should react the least rapidly of the four. Note that the reduction potentials of U (2'-deoxyuridine), uridine, and T are the same;<sup>18,19</sup> therefore, their ET quenching reactivities should also be similar.

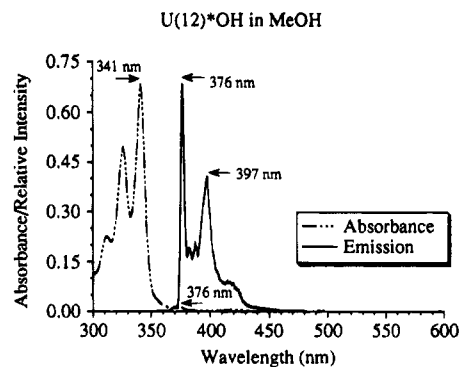


**Figure 2.** Absorbance and emission spectra for the U(12)\*OH (1) nucleoside in MeOH at concentrations of  $1.6 \times 10^{-5}$  and  $2.5 \times 10^{-6}$  M, respectively.

**Spectra and Emission Kinetics for U(12)\*-Nucleosides 1 and 2.** The low-energy electronic absorbance and the emission spectra for U(12)\*OH (1) in MeOH are plotted in Figure 2. These two spectra are virtually identical to those of PBA in either MeOH or phosphate buffer solution. The fluorescence originates from the lowest energy  $\pi, \pi^*$  electronic state and shows vibrational structure which is characteristic of many polyaromatic hydrocarbons (PAH). There is no evidence of intramolecular U/pyrene association in the ground state absorbance spectrum of this molecule. It is also important to note that the  $\pi, \pi^*$  fluorescence from U(12)\*OH (1) and U(12)\*ODMT (2) does not extend beyond ca. 460 nm. However, solutions of 1 and 2 in MeOH do emit weakly in the 460–500 nm range, and for solutions in the  $10^{-5}$ – $10^{-4}$  M concentration range laser-excited emission kinetics can be measured in this wavelength region (see below). Figure 3 presents plots of fluorescence decay and lifetime fit data for U(12)\*OH (1) in MeOH for a 200-ns time window at 400 and 495 nm. Data from both longer and shorter time windows (typically as long as 1–2  $\mu\text{s}$  and as short as 20–50 ns) were combined to produce the fluorescence lifetime data in Table 3.

It is well-known that photoexcited pyrene molecules can form excimers through complexation with a ground-state pyrene molecule. It is also true that the CT character of the pyrene excimer is responsible for its extremely broad emission centered in the 500-nm spectral region.<sup>30,99-104</sup> An upper limit for the bimolecular excimer formation constant for U(12)\*OH molecules is ca.  $2 \times 10^{10} \text{ M}^{-1} \text{ s}^{-1}$ .<sup>3</sup> Thus for concentrations  $\leq 1.2 \times 10^{-4}$  M, the bimolecular excimer formation time would be in excess of 400 ns. Figure 3 shows that for U(12)\*OH (1) at a concentration of  $1.2 \times 10^{-4}$  M in MeOH, there is an increase in emission in the 495-nm region with a lifetime of 25 ns. No similar increase in emission is seen at 400 nm for this same molecule (see Figure 3 and Table 3). Table 3 presents emission lifetime and quantum yield data for PBA, U(12)\*OH (1), and U(12)\*ODMT (2) in MeOH at 400 and 495 nm. Emission kinetics were also recorded for 1 and 2 at these two wavelengths at lower ( $1 \times 10^{-5}$  M) and higher ( $1 \times 10^{-4}$  M) concentrations (data not shown). An important observation that can be made from these data is that both the  $\pi, \pi^*$  fluorescence decay at 400 nm and the emission decay and increase kinetics at 495 nm are independent of sample concentration below  $1.2 \times 10^{-4}$  M. Thus the novel growth of emission at 495 nm in the 15–25 ns time range is due solely to an intramolecular process within U(12)\*-molecules. (Note that emission-growth lifetimes at 495 nm in Table 3 have negative amplitudes.) Additional data and arguments will be presented later in this paper, but our assignment of the 495-nm emission in U(12)\* molecules, which lack intramolecular ground-state complexation as U(12)\*OH and U(12)\*ODMT do, is that it arises from an intramolecular CT-

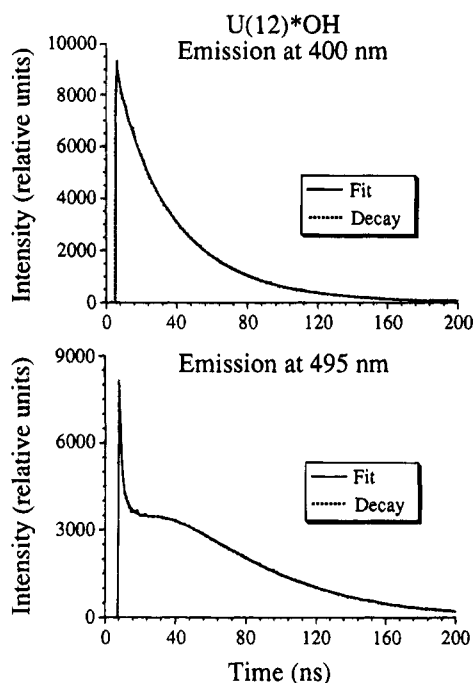


**Figure 3.** Plot of relative emission intensity versus time at 400 and 495 nm for the U(12)\*OH (1) nucleoside in MeOH. Top: 1 at a concentration of  $2.7 \times 10^{-5}$  M. The emission data are fit to the sum of three exponentials with lifetimes of 0.47, 14, and 38 ns;  $\chi^2 = 3.7$ ; 200 ns time range. The lifetimes reported in Table 3 for 1 at this wavelength are based on fits over several time ranges. Bottom: 1 at a concentration of  $1.2 \times 10^{-4}$  M. The emission data are fit to the sum of four exponentials with lifetimes [relative amplitudes] of 0.84 [0.33], 4.9 [0.14], 25 [-0.40], and 50 [0.53] ns;  $\chi^2 = 2.3$ ; 200 ns time range. The amplitude of the 25-ns component is negative indicating an increase in emission with this lifetime.

**TABLE 3: Emission Lifetime (ns) and Quantum Yield ( $\Phi_{em}$ ) Data for PBA, U(12)\*OH (1) and U(12)\*ODMT (2) in MeOH<sup>a</sup>**

molecule	400 nm	495 nm	$\Phi_{em}^b$
PBA <sup>c,d</sup> ( $9 \times 10^{-6}$ M)	[0.45] 125 (38%) [0.55] 231 (62%)		0.065
U(12)*OH (1) <sup>d</sup> ( $2.7 \times 10^{-5}$ M)	[0.39] 0.6 (1%) [0.16] 12 (10%) [0.45] 38 (89%) <250 (impurity)	[0.63] 0.4 (6%) [0.06] 2.7 (4%) [-0.22] 18 (18%) <sup>e</sup> [0.31] 51 (72%)	0.026
U(12)*ODMT (2) <sup>d</sup> ( $3.9 \times 10^{-5}$ M)	[0.39] 0.6 (2%) [0.15] 11 (11%) [0.46] 27 (87%) 270 (impurity)	[0.42] 0.5 (1%) [0.28] 7.3 (10%) [-0.22] 15 (17%) <sup>e</sup> [0.30] 50. (72%)	0.025

<sup>a</sup> Emission lifetimes were measured in O-ring-sealed sample cells which were vacuum degassed. Relative amplitudes in the emission decay fits are given before the lifetimes as decimal fractions in brackets; relative emission areas are given after the lifetimes as percentages in parentheses. <sup>b</sup> For PBA, measured relative to 9,10-diphenylanthracene in cyclohexane ( $\Phi_{em} = 1.0$ , see above); for 1 and 2, measured relative to PBA in MeOH. <sup>c</sup> Biexponential emission decay lifetimes of 95 ns (0.90 relative amplitude, 80% relative area) and 193 ns (0.10 relative amplitude, 20% relative area) were also observed in 7.5 mM borate buffer pH 9.0. <sup>d</sup> Concentrations for quantum yield measurements were ca.  $2.5 \times 10^{-6}$  M. <sup>e</sup> Negative emission lifetime amplitudes indicate an increase (or growth) in emission intensity.

excited state, pyrene<sup>+</sup>/U<sup>-</sup>. This type of state can also be referred to as an intramolecular heteroexciplex.

The emission quantum yield measured here for PBA in MeOH is 0.065, while those for 1 and 2 in MeOH are 0.026 and 0.025, respectively. There are also significant  $\pi, \pi^*$ -emission lifetime reductions in MeOH between PBA and the two pyrene-labeled nucleosides. PBA's emission in MeOH is

biexponential with lifetime components of 125 [0.45 relative emission amplitude] and 231 ns [0.55 relative emission amplitude]. The reason PBA emission in MeOH exhibits two lifetimes is not clear; however, it is not necessary to know this reason for this study. It is true, though, that when PBA is dissolved in aqueous phosphate buffer at pH 9.0, the lifetime pattern changes to the following, 95 ns [0.90 relative emission amplitude] and 193 ns [0.10 relative emission amplitude]. PBA's emission lifetime properties are presented here only to show the kind of behavior a 1-alkylpyrenyl ligand's  $\pi^*$  excited state might exhibit in the absence of ET quenching. In contrast to the long emission lifetimes of PBA, the kinetics data in Table 3 show that the  $\pi, \pi^*$  emission decays of 1 and 2 in MeOH are triexponential with longest lifetime components only ca. 38 and 27 ns, respectively.

Several more comments can be made concerning the emission data in Table 3. One, some long-lived (greater than 150 ns) impurity emission is seen in the 400-nm region where pyrene itself fluoresces. (HPLC purification procedures eliminate this impurity emission from the oligomers and duplexes discussed next.) The lifetime of this impurity emission is shortest (ca. 160 ns) at the highest concentrations (ca.  $10^{-4}$  M), where bimolecular quenching is expected to be observable on greater than 200-ns time scales. The lifetime of this impurity emission thus provides an internal check on the time range of bimolecular pyrene\*/pyrene interactions. Two, the substantial lifetime reductions for 1 and 2 relative to PBA are consistent with intramolecular ET quenching in these nucleosides. Three, the longest emission lifetime in U(12)\*ODMT (2) is only 70% as long as in U(12)\*OH (1). This is consistent with the DMT group in the former nucleoside reducing the range of motion (or free volume) accessible to the uridine and pyrene chromophores relative to their range of motion in the latter nucleoside. Four, the emission kinetics at 495 nm for both nucleosides are quadruply exponential with identical longest emission lifetimes of ca. 50 ns. Five, judging by the emission amplitudes at both 400 and 495 nm for both nucleosides, most of the emission decay occurs in two time ranges,  $\leq 1$  ns and  $\geq 25$  ns. This pattern for the  $\pi, \pi^*$  quenching at 400 nm suggests that only ca. one-sixth of the photoexcited nucleosides do not have relative uridine/pyrene configurations which are either close together or well separated. Six, for both U(12)\*-nucleosides a substantial (30–60%) amount of 495-nm emission decays in  $\leq 1$  ns.

At 495 nm in Table 3, the negative amplitudes of the 15–18 ns emission lifetime components for 1 and 2 indicate an increase rather than a decay in emission. This emission increase can reasonably be assigned to the formation of an emissive pyrene<sup>+</sup>/U<sup>-</sup> CT product with an emission maximum considerably to the red of the  $\pi, \pi^*$  emission from pyrene\*. However, it is unlikely that this CT product itself lives much longer than ca. 5–10 ns. The slightly longer longest-emission lifetimes at 495 nm than at 400 nm are most likely dominated by a rate-limiting pyrene\* ET quenching step. This model is also supported by a recent report in which pyrene<sup>+</sup>/U<sup>-</sup> CT emission is observed for the 5-(1-pyrenyl)-U nucleoside in MeOH.<sup>10</sup> There broad CT emission with maximum intensity at 475 nm is formed from the ET quenching of pyrene\* in less than 50 ps and decays with biexponential lifetimes of  $\leq 50$  and 900 ps. Note that for the 5-(1-pyrenyl)-U nucleoside in MeOH, ET quenching of pyrene\* emission is almost complete, and CT emission is present almost exclusively; however, switching solvent from MeOH to tetrahydrofuran eliminates CT emission and fully restores  $\pi, \pi^*$  emission.<sup>10</sup> A clear example of a CT emission band in a U(12)\*-labeled DNA system is presented in Figure 4.

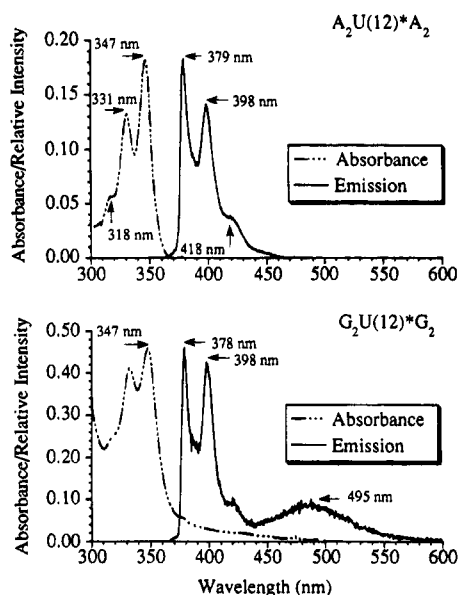


**Figure 4.** Absorbance and emission spectra in 7.5 mM monosodium phosphate buffer pH 7.0 with 1.0 M NaCl and 1 mM Na<sub>2</sub>EDTA. Top: the A<sub>2</sub>U(12)\*A<sub>2</sub> pentamer at concentrations of  $5.7 \times 10^{-6}$  M. Bottom: the G<sub>2</sub>U(12)\*G<sub>2</sub> pentamer at concentrations for absorbance and emission, respectively, of  $1.6 \times 10^{-5}$  and  $1.1 \times 10^{-6}$  M.

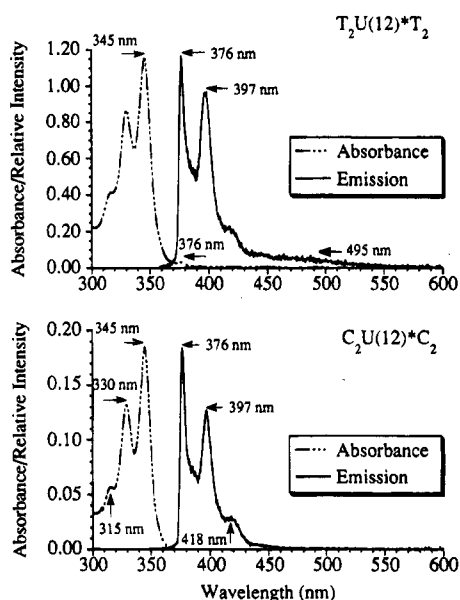


**Figure 5.** Absorbance and emission spectra in the same buffer as in Figure 4. Top: the T<sub>2</sub>U(12)\*T<sub>2</sub> pentamer at concentrations for absorbance and emission, respectively, of  $3.7 \times 10^{-5}$  and  $1.3 \times 10^{-6}$  M. Bottom: the C<sub>2</sub>U(12)\*C<sub>2</sub> pentamer at concentrations of  $5.6 \times 10^{-6}$  M.

**Spectra and Emission Kinetics for Four U(12)\*-Labeled Pentamers.** Figures 4 and 5 show ground-state absorbance and fluorescence spectra for four U(12)\*-labeled oligonucleotides with five nucleic acid bases each. In each of the four pentamers, U(12)\* is flanked symmetrically by a pair of homonucleotides. Although one central uridine is always available to quench pyrene\*, either the other four bases in each pentamer can competitively quench pyrene\* and thus cause more rapid loss of pyrene\* emission than in U(12)\*OH or they can block access to the central uridine and thus lengthen the lifetime of at least some of pyrene\* emission. As a result the emission lifetimes in each of the oligomers can serve as a monitor of the reactivity of the flanking bases, and an ordering of the relative reactivities of each of the four DNA nucleosides can be obtained. If ET quenching by DNA bases is the dominant mode of pyrene\*

**TABLE 4: Emission Lifetime (ns) Data for Four U(12)\*-Labeled Polynucleotides in Aqueous Buffer<sup>a</sup>**

U(12)*-pentamer	400 nm	495 nm
A <sub>2</sub> U(12)*A <sub>2</sub> <sup>b</sup>	[0.26] 5.9 (4%) [0.38] 30. (29%) [0.33] 64 (53%) [0.03] 200. (14%)	{trace emission only}
average lifetime	40 ns	
G <sub>2</sub> U(12)*G <sub>2</sub> <sup>c</sup>	[0.58] 1.7 (11%) [0.28] 8.3 (26%) [0.13] 30. (46%) [0.01] 108 (17%)	[0.40] 0.7 (2%) [0.28] 10. (16%) [0.20] 33 (37%) [0.12] 63 (45%)
average lifetime	8.3 ns	
T <sub>2</sub> U(12)*T <sub>2</sub> <sup>d</sup>	[0.81] 0.2 (13%) [0.09] 1.5 (12%) [0.07] 5.3 (31%) [0.03] 20. (44%)	[0.79] 0.1 (11%) [0.16] 1.3 (34%) [0.05] 6.8 (55%)
average lifetime	1.3 ns	
C <sub>2</sub> U(12)*C <sub>2</sub> <sup>e</sup>	[0.71] 0.14 (15%) [0.25] 1.3 (50%) [0.04] 5.6 (35%)	{trace emission only}
average lifetime	0.6 ns	

<sup>a</sup> Emission lifetimes were measured in 7.5 mM monosodium phosphate buffer pH 7.0 with 1.0 M NaCl and 1 mM Na<sub>2</sub>EDTA in O-ring-sealed sample cells which were vacuum degassed. The same data conventions as in Table 3 are used here. Average lifetime is the sum of the products of the amplitudes and lifetimes. <sup>b</sup> Concentration =  $6.1 \times 10^{-6}$  M. The emission decay kinetics for this sample require more than four lifetimes to fit the data if all time scales from 50 to 1000 ns are considered. Limiting the analysis to four lifetimes by considering data only from the longer time ranges, yields the lifetimes in this table. In fact emission decays with lifetimes  $\leq 2$  ns also appear to be present on the shortest time scales. <sup>c</sup> Concentration =  $1.6 \times 10^{-5}$  M.  $\Phi_{em} = 2.2 \times 10^{-2}$  measured relative to PBA in phosphate buffer ( $\Phi_{em} = 0.60$ , see above). <sup>d</sup> Concentration =  $3.7 \times 10^{-5}$  M.  $\Phi_{em} = 8.6 \times 10^{-4}$  measured relative to PBA in the phosphate buffer. <sup>e</sup> Concentration =  $3.0 \times 10^{-5}$  M.

deactivation in these oligomers, one would expect the following order of increasing reactivity for flanking nucleotides based on the above  $\Delta G^\circ(ET)$  estimates; A < G < T  $\approx$  C.

The absorbance and emission spectra of A<sub>2</sub>U(12)\*A<sub>2</sub> (Figure 4, top) are very similar to those of PBA and of the U(12)\*-nucleosides. Additionally, Table 4 shows that at least a small percentage of pyrene\*/uridine configurations are sufficiently well separated that they have excited state lifetimes of ca. 200 ns at 400 nm. Such long emission lifetimes are comparable to those of the longest emission components of PBA in MeOH and aqueous buffer solutions and significantly greater than the 30–40 ns longest emission lifetimes of the U(12)\*-nucleosides 1 and 2; they indicate uridine-blocking by unreactive adenosine nucleosides. Too little 495-nm emission was present for reliable lifetime measurements to be made at this wavelength. Finally, only about 25% of the emission amplitude of this pentamer decays in  $\leq 6$  ns. Thus its relative fraction of close pyrene\*/uridine configurations is not very large. In contrast to the U(12)\*-nucleoside samples, HPLC purification of the oligomeric DNA samples removed all fluorescent pyrene impurities (see especially the 400-nm lifetime data in Table 4 for the T<sub>2</sub>U(12)\*T<sub>2</sub> and C<sub>2</sub>U(12)\*C<sub>2</sub> pentamers).

The absorbance and emission spectra of G<sub>2</sub>U(12)\*G<sub>2</sub> in the bottom of Figure 4 show some striking differences when compared to those just discussed for A<sub>2</sub>U(12)\*A<sub>2</sub>. One important new feature is the broad CT emission centered in the 495-nm region. The ground-state absorbance spectrum also shows extensive red-shifting and blurring of the pyrene chromophore's vibrational fine structure. Other workers have noted the tendency of guanine to form ground-state complexes with pyrene.<sup>3,105</sup> The red-shifted ground-state absorbance is consis-

tent, therefore, with intramolecular association of the pyrene and guanine subunits within this pentamer. Table 4 shows that the longest emission lifetime present in this pentamer is ca. 108 ns. Additionally, ca. 60% of the emission amplitude decays within the first 2 ns. Both of these results are indicative of greater reactivity for flanking G nucleotides than for flanking A nucleotides. This finding is in accord with the expectation (see Table 1) that  $\Delta G^\circ$  for reductive quenching of pyrene\* by G is negative,  $-0.33$  eV. The lifetime of the emission at 495-nm extends to ca. 63 ns. However, the red-shifted ground-state absorbance for the pyrene label in  $G_2U(12)^*G_2$  indicates that the emission at 495 nm is likely due to both  $\pi,\pi^*$ -emission from intramolecular guanine/pyrene\* complexes and CT-emission from the pyrene<sup>+</sup>/U(12)<sup>-</sup> CT product.

The emission spectrum of  $T_2U(12)^*T_2$  in the top of Figure 5 shows some 495-nm emission whose intensity relative to the  $\pi,\pi^*$  emission is intermediate between that of  $A_2U(12)^*A_2$  and  $G_2U(12)^*G_2$ . Table 4 shows that the lifetime of this emission is triexponential with the longest component living only 6.8 ns. Note also that ca. 80% of the 495-nm emission decays in less than 0.2 ns; the same is also true of the 400-nm emission originating from the  $\pi,\pi^*$  excited state. In accord with the very negative free-energy change expected for thymidine and uridine ET quenching of pyrene\* emission,  $-0.52$  eV, the longest emission lifetime component at 400 nm lives only 20 ns. Additionally ca. 90% of the 400-nm emission amplitude decays in less than 2 ns for this pentamer, while for  $G_2U(12)^*G_2$  ca. 60% of the 400-nm emission decays in this same time period.

Several comparisons of the relative pyrene\* quenching reactivities between the  $G_2U(12)^*G_2$  and  $T_2U(12)^*T_2$  pentamers are possible, and all support the conclusion that flanking G nucleotides are significantly less reactive than are flanking T nucleotides. First, the longest  $\pi,\pi^*$  emission component at 400 nm for the former is 108 ns and for the latter is 20 ns. Second, the relative emission amplitudes and their corresponding lifetimes can be used to calculate an average emission lifetime for each pentamer. This yields average lifetimes of 8.3 and 1.3 ns, respectively, for flanking G and T nucleotides. Third, the emission quantum yields for these two pentamers are, respectively,  $2.2 \times 10^{-2}$  and  $8.6 \times 10^{-4}$  for  $G_2U(12)^*G_2$  and  $T_2U(12)^*T_2$ . In this regard it is worth noting that  $G_2U(12)^*G_2$  emits about 27-fold less light than does PBA in the same buffer, and  $T_2U(12)^*T_2$  emits about 25-fold less light than does  $G_2U(12)^*G_2$ . The ratios of average lifetimes give only a 6-fold lowering on going from flanking G to flanking T nucleotides, but the amount of  $\leq 0.2$  ns emission in the  $T_2U(12)^*T_2$  pentamer is very likely underestimated (see below).

Comparison of the ground-state absorbance spectra among the four pentamers in Figures 4 and 5 shows that  $G_2U(12)^*G_2$  is unique in having an absorbance spectrum which has both a strong red-shift and significantly reduced vibrational fine structure. However, both  $G_2U(12)^*G_2$  and  $T_2U(12)^*T_2$  pentamers show 495-nm emission. The emission spectrum of  $C_2U(12)^*C_2$  in the bottom of Figure 5 is very much like that of PBA, the U(12)\*-nucleosides 1 and 2, and  $A_2U(12)^*A_2$ . However, the lifetime data in Table 4 for this pentamer show it to be unique in that its longest emission-lifetime component lives only 5.6 ns. Also, ca. 95% of its emission is quenched in less than 1.5 ns. These data show that flanking C nucleosides are even more reactive toward pyrene\* quenching than are flanking T nucleosides. If pyrene\* quenching produces C(H)\*, it establishes an upper limit for the time of protonation of C<sup>-</sup> as less than 0.2 ns. For the case of pyrene\* ET quenching by T in  $T_2U(12)^*T_2$ , CT emission from the pyrene<sup>+</sup>/U(12)<sup>-</sup> (and possibly also from pyrene<sup>+</sup>/T<sup>-</sup>) product is seen. However,

**TABLE 5: Four U(12)\*-Labeled DNA Duplexes and Their  $T_m$  Values**

oligonucleotide strands mixed	$T_m^a$	duplex identifier
V and Vc	55	18/AAU(12)*
VI and VIc	65	18/GGU(12)*
VII and VIIc	54	18/TTU(12)*
VIII and VIIIc	64	18/CCU(12)*

<sup>a</sup> The duplex concentrations for the first and fourth duplexes were  $5.9 \times 10^{-6}$  M and for the second and third were  $3.4 \times 10^{-6}$  M. All samples were suspended in the same buffer as in Figure 4. See Table 1 for the base sequences of each strand.

for the case of ET quenching by C in  $C_2U(12)^*C_2$ , no 495-nm CT emission is found. Either the pyrene<sup>+</sup>/C<sup>-</sup> product does not emit or its lifetime is extremely short. No 495-nm emission is found for the  $A_2U(12)^*A_2$  pentamer either. However, in this case the 400-nm  $\pi,\pi^*$  emission from pyrene\* is very long lived (as long as ca. 200 ns). Here lack of CT emission is consistent with domination of the short-lived pyrene<sup>+</sup>/U(12)<sup>-</sup> emission by the much longer lived emission from slowly unquenched  $\pi,\pi^*$  states.

**Spectra and Thermodynamics of U(12)\*-Labeled Duplexes.** The above kinetics studies on pentameric oligonucleotides establish the following order of pyrene\* quenching reactivities for flanking pairs of DNA bases:  $A < G < T < C$ . All other factors being unchanged, one would expect the same pattern of quenching reactivities in correspondingly constructed DNA duplexes. However, the relatively fixed structure of ds DNA significantly restricts the exposure of the nucleic acid bases to covalently attached pyrene\*. A complication in ds DNA studies is the possibility of pyrene\* quenching by across-strand as well as by same-strand bases. One simplification is available in this work; namely, A nucleotides are unreactive. Thus they can be used as insulators, and both across-strand and same-strand effects can be cleanly established for flanking T nucleotides. Table 5 lists the U(12)\*-labeled strands which were mixed in equimolar amounts to produce the four DNA duplexes studied.

Several points can be made concerning the  $T_m$  data and the base sequences of the duplexes listed in Tables 1 and 5. Each of the four duplexes is 18 bp long so that the duplexes without G/C base pairs would have high enough  $T_m$  values that less than 1% of the duplexes would be melted (or in the ss configuration) at room temperature. The  $T_m$  is the temperature at which 50% of a sample of ds DNA is melted into ss oligomers. For the 18/AAU(12)\* and 18/TTU(12)\* pair of duplexes, each contains the same number of bases but differs from the other due strand-interchange of the four U(12)\*-flanking nucleotides. This is also true for the 18/GGU(12)\* and 18/CCU(12)\* pair of duplexes. Both duplexes within each of these pairs have the same  $T_m$  values. Finally, the third base on either side of U(12)\* is an adenine, which does not quench pyrene\* emission. Thus the nearest same-strand base-quencher which can compete with pyrene\*-quenching by the four U(12)\*-flanking nucleotides is a T ca. 13 Å away.

Figure 6 shows absorbance and emission spectra for the 18/AAU(12)\* duplex. The dominance of the DNA absorbance at 260 nm over that of the pyrene label at 351 nm is readily apparent. The clear separation of the DNA and pyrene label absorbances means that pyrene can be photoexcited without exciting DNA and that the absorbance and emission spectra of the pyrene label can be studied as arising from an isolated chromophore. The fluorescence tail beyond 460 nm for 18/AAU(12)\* is present for the other three duplexes and looks much the same. Note that this extended red-emission was not

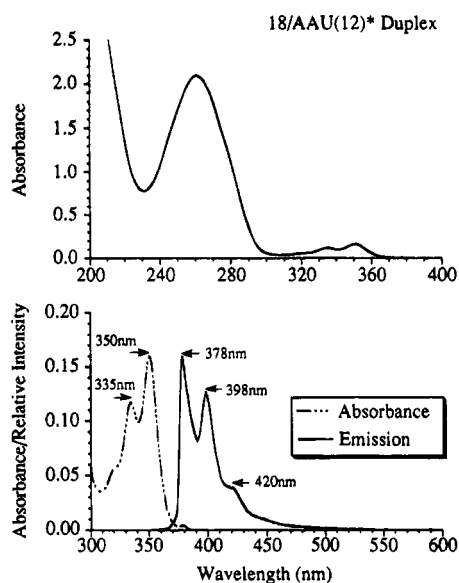


**Figure 6.** Absorbance and emission spectra for the 18/AAU(12)\* duplex in the same buffer as in Figure 4 at concentrations of  $5.9 \times 10^{-6}$  M in duplex. Top: an absorbance spectrum in the 200–400 nm range. Bottom: absorbance and relative emission spectra in the 300–600 nm range.

seen for U(12)\*OH (Figure 2) or for two of the pentamers studied, A<sub>2</sub>U(12)\*A<sub>2</sub> and C<sub>2</sub>U(12)\*C<sub>2</sub> (Figures 4 and 5). Additionally, the absorbance spectra of three duplexes, 18/AAU(12)\*, 18/TTU(12)\*, and 18/CCU(12)\*, are essentially the same. The ground state absorbance of 18/GGU(12)\*, however, is similar to that of the corresponding pentamer, G<sub>2</sub>U(12)\*G<sub>2</sub>, with red-shifted absorbance extending as far as 450 nm. Neither the 18/GGU(12)\* nor 18/TTU(12)\* duplexes, however, show the pronounced 495-nm region emission that is seen in the corresponding pentamers (see Figures 4 and 5).

Absorbance versus temperature ( $T_m$ ) curves were measured at 260 nm for the four duplexes listed in Table 5 and verify the expected, reversible formation of ds conformations as a function of temperature. In addition each was well fit by a two-state (all or nothing) duplex formation model.<sup>41,42</sup> The  $T_m$  values listed in Table 5 were obtained from nonlinear least-squares fits of the two-state model to the experimental absorbance versus temperature data. CD spectra were measured for the 18/TTU(12)\* and 18/GGU(12)\* duplexes and show normal B-form DNA spectra with negative and positive bands in the 230–290 nm region.<sup>106–109</sup>

**Kinetics of U(12)\*-Labeled Duplexes.** Table 6 presents emission lifetime data for the four U(12)\*-labeled duplexes listed in Table 5. All of these duplexes show emission decays in the 495-nm region while only two of the four pentamers do (G<sub>2</sub>U(12)\*G<sub>2</sub> and T<sub>2</sub>U(12)\*T<sub>2</sub>). Additionally, at 495 nm all four of these duplexes have remarkably similar three-component exponential decay lifetimes and amplitudes in the  $\leq 6$  ns time range: 70–85% of the amplitude decays in less than 1 ns and 15–30% decays in 1–6 ns. Only the 18/GGU(12)\* duplex shows longer 495-nm emission decay (22 ns). This exception is consistent with the red-shifted absorbance spectrum of this duplex and is likely due to some  $\pi, \pi^*$  emission extending into the 495-nm region.

As noted above the lifetimes and amplitudes of ultrashort-lifetime components (less than 0.5 ns) with small relative emission areas (less than 10%) are very uncertain. One way to deal with this and still generate a lifetime-based pyrene\* quenching reactivity index is to consider only lifetimes which are  $\geq 1$  ns. At 400 nm for the four duplexes in Table 6, 91–

**TABLE 6: Emission Lifetime (ns) Data for Four U(12)\*-Labeled DNA Duplexes in Aqueous Buffer<sup>a</sup>**

DNA duplex	400 nm	495 nm
18/AAU(12)* <sup>b</sup>	[0.17] 0.5 (<1%) [0.37] 5.3 (11%) [0.36] 21 (44%) [0.10] 75 (45%)	[0.69] 0.1 (8%) [0.13] 1.6 (17%) [0.18] 5.4 (75%)
average lifetime	21 ns	
18/GGU(12)* <sup>c</sup>	[0.72] 0.4 (8%) [0.16] 3.0 (14%) [0.10] 17 (48%) [0.02] 59 (30%)	[0.67] 0.2 (14%) [0.22] 1.2 (28%) [0.09] 5.4 (49%) [0.02] 22 (9%)
average lifetime	12 ns	
18/TTU(12)* <sup>d</sup>	[0.81] 0.4 (9%) [0.11] 3.3 (10%) [0.06] 18 (29%) [0.02] 97 (52%)	[0.73] 0.2 (21%) [0.22] 0.81 (30%) [0.05] 6.5 (49%)
average lifetime	18 ns	
18/CCU(12)* <sup>e</sup>	[0.68] 0.4 (9%) [0.18] 2.7 (17%) [0.08] 18 (45%) [0.06] 65 (29%)	[0.85] 0.1 (14%) [0.08] 1.6 (20%) [0.07] 5.5 (66%)
average lifetime	18 ns	

<sup>a</sup> Emission lifetimes were measured phosphate buffer under the same conditions as in Table 4. The same data conventions as in Table 3 are used here. Average lifetime is the sum of the products of amplitude and lifetime for the greater than 1 ns components divided by the sum of these amplitudes. <sup>b</sup> Concentration =  $1.1 \times 10^{-5}$  M. <sup>c</sup> Concentration =  $1.7 \times 10^{-5}$  M.  $\Phi_{em} = 9.1 \times 10^{-3}$  measured relative to PBA in the phosphate buffer. <sup>d</sup> Concentration =  $1.2 \times 10^{-5}$  M.  $\Phi_{em} = 1.7 \times 10^{-2}$  measured relative to PBA in the phosphate buffer. <sup>e</sup> Concentration =  $1.3 \times 10^{-5}$  M.

99% of the emission area is due these components. When the normalized average of these emission lifetimes (normalized so that the sum of the greater than 1-ns components has unity emission amplitude) is calculated as shown in Table 6, all four of the duplexes have very similar average lifetimes. Support for the reasonableness of this calculation method comes from noting that the apparent 33% reduction in average lifetime on going from 18/TTU(12)\* to 18/GGU(12)\*, 18 to 12 ns, is reflected in a 46% reduction in measured emission quantum yield, 0.017 to 0.0091, for these same two duplexes.

Despite the fact that in the  $\pi, \pi^*$  region at 400 nm the averages of the greater than 1-ns lifetimes for the 18/GGU(12)\* and 18/CCU(12)\* duplexes differ, respectively 12 and 18 ns, the emission decay amplitudes, lifetimes, and even the fractional areas for these two duplexes are remarkably similar. Since pyrene\* quenching by C greatly exceeds that by G (see Table 4), the similarity of  $\pi, \pi^*$  quenching for these two duplexes most likely results from similar pyrene\*-quenching rates by C nucleotides for both same-strand and across-strand positions. In view of this, it is a little surprising that 18/GGU(12)\* shows red-shifted ground-state absorbance while 18/CCU(12)\* does not. However, the 400- and 495-nm emission kinetics data suggest that the majority of  $\geq 1$  ns pyrene\*/DNA interactions are quite similar in these two duplexes.

Table 4 shows that U(12)\*-flanking A nucleotides are unreactive with respect to pyrene\* quenching while flanking T nucleotides are very reactive. Thus differences in emission kinetics at 400 nm between the 18/AAU(12)\* and 18/TTU(12)\* duplexes are likely to reflect same-strand versus across-strand pyrene\*-quenching differences by flanking T nucleotides. The 18/TTU(12)\* duplex shows ca. 81% emission amplitude decay in  $\leq 1$  ns, while the 18/AAU(12)\* one shows only ca. 17% amplitude decay in the same time range. This likely reflects a different distribution of pyrene\*/DNA conformations in these two duplexes. The same-strand flanking T nucleotides appar-

ently produce many more closely associated pyrene\*/DNA conformers than do the across-strand T nucleotides. Another difference between them is that ca. 46% of the emission amplitude lasts longer than 20 ns for 18/AAU(12)\*, but only ca. 8% lasts comparably long in 18/TTU(12)\*. By considering only lifetime components which are greater than 1-ns long, the subnanosecond "static-quenching" effects of closely associated pyrene\*/DNA conformers are masked, and correspondingly the pyrene\* quenching effects of more loosely associated pyrene\*/DNA conformers are emphasized. From this perspective the 18/AAU(12)\* and 18/TTU(12)\* duplexes have the same average lifetimes and very similar individual lifetime components.

## Discussion

PBA is reasonable model for the quantum yield of a 1-alkylpyrenyl chromophore in phosphate buffer, and its quantum yield is 0.60 in air-equilibrated solution. In contrast the quantum yields of 18/TTU(12)\* and 18/GGU(12)\* are, respectively, 0.017 and 0.0091 in argon-bubbled solution, 35–66-fold less than that of PBA. Because 98% of the emitting species decay in less than 20 ns for these two duplexes, there should not be much difference between their quantum yields in air-equilibrated, FPT-prepared, or argon-bubbled samples. Thus, it is also true that the implied radiative lifetime for the pyrene\*-label in these two duplexes is in the 200–400 ns range (average lifetime based on all components/emission quantum yield). This accords with the longest emission lifetimes found for PBA in MeOH and the A<sub>2</sub>U(12)\*A<sub>2</sub> pentamer in phosphate buffer. It also agrees with the implied radiative lifetime of G<sub>2</sub>U(12)\*G<sub>2</sub> in buffer, 380 ns (8.3 ns/0.022). The single exception is the implied radiative lifetime of T<sub>2</sub>U(12)\*T<sub>2</sub> which is ca. 4 times longer than this range. This is likely due to an underestimate of the amplitude of ultrafast (less than 0.2 ns) quenching in this pentamer. An important corollary of this comparison of average lifetimes and emission quantum yields is that, except for a few ultrafast components such as that just mentioned, the amplitudes of the lifetime components present reasonable estimates of the relative fractions of emitting species present in a sample for each lifetime.

Additional confidence in the calculated radiative lifetimes for pyrene\* labels in U(12)\*-containing duplexes comes from measurements of the radiative lifetime of PBA in acetonitrile and in buffer. In air-equilibrated acetonitrile a single emission lifetime of 15.4 ± 0.3 ns is found at 380, 400, and 420 nm, and the emission quantum yield is 0.056 ± 0.004. These data imply a radiative lifetime of 275 ± 25 ns for PBA in this solvent. In the same phosphate buffer as used for the emission lifetime studies of U(12)\*-labeled pentamers and duplexes, however, air-equilibrated PBA has two emission lifetimes which vary in relative amplitude with wavelength. The lifetimes are 14.3 ± 0.3 and 94 ± 4 ns, and the relative emission amplitude of the shorter lifetime increases from 7% to 32% as wavelength is varied from 380 to 420 nm. Thus the radiative lifetime calculated using the longer emission component is probably a lower limit, 156 ns (94 ns/0.60). Nevertheless, both of these results for PBA suggest that a radiative lifetime of 200–400 ns for pyrene\* labels on DNA oligomers and duplexes is reasonable.

Compared to pyrene\*-quenching by flanking T nucleotides in the T<sub>2</sub>U(12)\*T<sub>2</sub> pentamer both 18/AAU(12)\* and 18/TTU(12)\* duplexes show emission decay at much longer times: 2% amplitude each at 75 and 97 ns for the respective duplexes versus 3% amplitude at 20 ns for the single-strand pentamer. This likely reflects decreased access for some pyrene\* labels to the central base-paired T and U nucleotides

in the duplexes compared to pyrene\* access to the T and U nucleotides in the pentamer. Lengthened emission lifetimes in the 18/GGU(12)\* and 18/CCU(12)\* duplexes compared to the C<sub>2</sub>U(12)\*C<sub>2</sub> pentamer are even more dramatic: 12–14% amplitude at ≥ 17 ns for the duplexes versus 4% amplitude at 5.6 ns for the pentamer. Noting that at 400 nm average emission lifetimes (for greater than 1-ns components) lengthen from 5.8 to 18 ns, 3-fold, on going from T<sub>2</sub>U(12)\*T<sub>2</sub> to 18/TTU(12)\* and from 1.9 to 18 ns, 9-fold, on going from C<sub>2</sub>U(12)\*C<sub>2</sub> to 18/CCU(12)\* provides a measure of duplex-induced restricted access to ds DNA bases by loosely associated pyrene\* labels. In a recent experiment with a 5-atom linker joining a 1-alkylpyrene label (pyr) to the 5'-end of an RNA-pentamer (pyr<sup>5</sup>CCUCU<sup>3</sup>), a 21-fold increase in pyrene\* emission was found when the pentamer bound to a mating ribozyme (catalytic RNA) internal guide sequence (5'GGAGGG<sup>3</sup>).<sup>40</sup>

Broad fluorescence at 460 nm similar to the 495-nm emission observed here for U(12)\*-labeled oligomers and duplexes has been reported for covalent adducts of the carcinogenic polycyclic hydrocarbon (+)-*anti*-benzo[*a*]pyrene-7,8-dihydrodiol-9,10-epoxide (BPDE) in polynucleotide duplexes.<sup>5,7,8,30,76,110</sup> However, the duplexes had multiple BPDE adducts, and the 460-nm emission was ascribed to pyrene\*/pyrene excimer formation. This conclusion contrasts with the CT assignment of the 495-nm emission described here. However, here only one pyrene label is present in each of the U(12)\* oligomers and duplexes; thus pyrene\*/pyrene excimers can be ruled out because of the low sample concentrations used. More relevant is the recent report for the 5-(1-pyrenyl)-U nucleoside of broad CT emission in MeOH with a maximum at 475 nm. The CT emission has a formation time of ≤ 50 ps and relaxes with biexponential decays of ≤ 50 and 0.9 ns.<sup>10</sup> Also relevant is the report of CT (or heteroexcimer) emission in a PAH/nucleoside adduct formed from the covalent binding of the carcinogen 2-aminofluorene (AF) to the C8 position of G to make G-C8-AF.<sup>111</sup> At room temperature, this adduct's fluorescence is broad and structureless with a maximum at 460 nm in aqueous solutions, shifting to 415 nm in solvents of lower polarity. In water a single short lifetime of 0.08 ns is seen. At 77 K this adduct's emission is structured and characteristic of π,π\* emission from AF. Note, however, the ET product in G-C8-AF is G<sup>•+</sup>/AF<sup>•-</sup>,<sup>1,3,21</sup> while in the 5-(1-pyrenyl)-U nucleoside it is pyrene<sup>•+</sup>/U<sup>•-</sup>.<sup>10</sup>

This work shows that for U(12)\*-nucleosides and the T<sub>2</sub>U(12)\*T<sub>2</sub> pentamer new emission decay kinetics and spectra are present in the 495-nm spectral region that are absent in PBA. These red emissions are ascribed to formation and decay of the CT-product, pyrene<sup>•+</sup>/U(12)<sup>•-</sup>. However, in the G<sub>2</sub>U(12)\*G<sub>2</sub> pentamer and in the 18/GGU(12)\* duplex both red-shifted ground-state absorbances and longer-lived 495-nm emission decays which are not characteristic of the pyrene<sup>•+</sup>/U(12)<sup>•-</sup> CT product are seen. For the G<sub>2</sub>U(12)\*G<sub>2</sub> pentamer, the 495-nm emission decay kinetics are much longer than those found for the T<sub>2</sub>U(12)\*T<sub>2</sub> pentamer. By way of contrast, the 495-nm emission decay kinetics of the 18/GGU(12)\* duplex are very similar to those of the 18/TTU(12)\* duplex.

The emission spectra in Figures 2, 4, and 5 for U(12)\*OH (1), A<sub>2</sub>U(12)A<sub>2</sub>, and C<sub>2</sub>U(12)\*C<sub>2</sub>, respectively, show that for these compounds π,π\* emission is much stronger than CT emission: as for PBA there is almost no observable emission for these complexes in the 450–550 nm region. In contrast, for two of the pentamers, T<sub>2</sub>U(12)\*T<sub>2</sub> and G<sub>2</sub>U(12)\*G<sub>2</sub>, CT emission is relatively strong compared to π,π\* emission, and emission in the 450–550 nm region is clearly observable under standard conditions (see Figures 4 and 5). The situation for all four of the duplexes studied here is intermediate between these

two cases with CT emission weak relative to  $\pi,\pi^*$  emission, but nevertheless emission in the 450–550 nm region is detectable (see Figure 6). Importantly, the lifetime data in Table 6 confirm that at 495-nm for the U(12)\*-labeled duplexes the emission lifetimes do not correspond to those of the  $\pi,\pi^*$  emission in the 400-nm region.

It is worth commenting in light of the above results and discussion, that experiments involving multiple PAH adducts (or labels) on DNA duplexes and single strands must now consider at least three types of photochemical processes: (1) differential ET quenching of PAH\* emission by nucleic acid bases, (2) formation of luminescent PAH/DNA CT products, and (3) formation of PAH\*/PAH excimers. For example, the absence of excimer emission in a duplex with multiple PAH adducts could be due either to improperly positioned adducts or to the fact that PAH\* emission is rapidly quenched by nearby bases.

### Conclusions

The 400-nm emission kinetics for the four U(12)\*-labeled pentamers establish the following order of pyrene\*-quenching reactivities by flanking DNA bases: A < G < T < C. This ordering of pyrene\*-quenching reactivities is generally consistent with estimates of the free energies of pyrene\*-quenching by ET to or from DNA bases. In the case of G nucleosides, pyrene\* is expected to be reduced; in the case of T, U, and C nucleosides, pyrene\* is expected to be oxidized. The shortened emission lifetimes in MeOH for the U(12)\*OH (1) and U(12)\*ODMT (2) nucleosides (30–40 ns) compared to that found for PBA in the same solvent (230 ns) are also consistent with ET quenching of pyrene\* by the covalently attached uridine to form pyrene<sup>•+</sup>/U(12)<sup>•-</sup>. Finally, emission spectra and lifetimes in the 495-nm region for both U(12)\*-labeled pentamers and duplexes provide direct evidence for the formation and decay of the pyrene<sup>•+</sup>/U(12)<sup>•-</sup> CT product. In general only ca. 20% of this CT-emission decays in the 1–7 ns time range with ca. 70–80% of it decaying in  $\leq 0.2$  ns.

Emission kinetics results for U(12)\*-labeled duplexes show that pyrene\*-quenching by pairs of flanking C and T nucleotides is equally effective both with respect to type of nucleotide and with respect to whether these nucleotides are located on the same strand as the U(12)\* label or on the opposite strand. Additionally, the longest  $\pi,\pi^*$  emission lifetimes in duplexes exceed those in the corresponding pentamers. This likely reflects restricted access of pyrene\* to the base-paired nucleotides in DNA duplexes compared to access to them in ss oligomers. A measure of duplex-induced restricted access to bases in ds versus ss DNA can be obtained by noting that the average  $\pi,\pi^*$  emission lifetimes (greater than 1-ns components) lengthen 3-fold on going from the T<sub>2</sub>U(12)\*T<sub>2</sub> pentamer to the 18/TTU(12)\* duplex and 9-fold on going from the C<sub>2</sub>U(12)\*C<sub>2</sub> pentamer to the 18/CCU(12)\* duplex.

The C<sub>2</sub>U(12)\*C<sub>2</sub> pentamer has a uniquely short emission decay with its longest emission-lifetime component lasting only 5.6 ns. Also, the average emission lifetimes for the C<sub>2</sub>U(12)\*C<sub>2</sub> and T<sub>2</sub>U(12)\*T<sub>2</sub> pentamers are respectively 1.9 and 5.8 ns. These data show that flanking C-nucleotides are somewhat more reactive toward pyrene\* quenching than are flanking T-nucleotides. This result is a little surprising because the free energies of ET quenching for both C and T nucleotides are similar, ca. -0.52 eV. However, it does not conflict with this fact, because other factors such as the sizes of the corresponding nuclear reorganization energies or the details of how proton transfer processes may be coupled to ET quenching in these two cases could account for the modestly higher quenching rate of flanking C over flanking T nucleotides.

**Acknowledgment.** M.M. and K.L.T. are indebted to Dr. P. Dan Cook for his guidance and support. The work at Georgia State University was supported by a grant to T.L.N. from the United States Department of Energy, Office of Health and Environment, Radiological and Chemical Physics Research Division (Grant No. DE-FG05-03ER61604 A002). T.L.N. acknowledges helpful conversations with Drs. David Wilson, Bruce Eaton, and Alex Siemiarczuk.

### References and Notes

- (1) Shafirovich, R. Y.; Levin, P. P.; Kuzmin, V. A.; Thorgeirsson, T. E.; Kliger, D. S.; Geacintov, N. E. *J. Am. Chem. Soc.* **1994**, *116*, 63.
- (2) Geacintov, N.; Prusik, T.; Khosroffian, J. *J. Am. Chem. Soc.* **1976**, *98*, 6444.
- (3) Geacintov, N. E.; Zhao, R.; Kuzmin, V. A.; Seog, K. K.; Pecora, L. *J. Photochem. Photobiol.* **1993**, *58*, 185.
- (4) Margulis, L.; Pluzhnikov, P. F.; Mao, B.; Kuzmin, V. A.; Chang, Y. J.; Scott, T. W.; Geacintov, N. E. *Chem. Phys. Lett.* **1991**, *187*, 597.
- (5) Eriksson, M.; Norden, B.; Jernstrom, B.; Graslund, A.; Lycksell, P.-O. *J. Chem. Soc., Chem. Commun.* **1988**, 211.
- (6) Eriksson, M.; Eriksson, S.; Jernstrom, B.; Norden, B.; Graslund, A. *Biopolymers* **1990**, *29*, 1249.
- (7) Vahakangas, K.; Yrjanheikki, E. *IARC Sci. Publ.* **1990**, *104*, 199.
- (8) Weston, A.; Bowman, E. D. *Carcinogenesis* **1991**, *12*, 1445.
- (9) O'Connor, D.; Shafirovich, V. Y.; Geacintov, N. *J. Phys. Chem.* **1994**, *98*, 9831.
- (10) Netzel, T. L.; Zhao, M.; Nafisi, K.; Headrick, J.; Sigman, M. S.; Eaton, B. E. *J. Am. Chem. Soc.* **1995**, *117*, 9119.
- (11) Sutin, N. In *Electron Transfer in Inorganic, Organic, and Biological Systems*; Bolton, J. R., Mataga, N., McLendon, G., Eds.; American Chemical Society: Washington, D.C., 1991; p 25.
- (12) Miller, J. R. In *Electron Transfer in Inorganic, Organic, and Biological Systems*; Bolton, J. R., Mataga, N., McLendon, G., Eds.; American Chemical Society: Washington, D.C., 1991; p 265.
- (13) Oevering, H.; Paddon-Row, M. N.; Heppener, M.; Oliver, A. M.; Cotsaris, E.; Verhoeven, J. W.; Hush, N. S. *J. Am. Chem. Soc.* **1987**, *109*, 3258.
- (14) Farid, R. S.; Fox, L. S.; Gray, H. B.; Kozik, M.; Chang, I. J.; Winkler, J. R. *Mol. Cryst. Liq. Cryst.* **1991**, *194*, 259.
- (15) Winkler, J. R.; Gray, H. B. *Chem. Rev.* **1992**, *92*, 369.
- (16) Wasielewski, M. R.; O'Neil, M. P.; Gosztola, D.; Niemczyk, M. P.; Svec, W. A. *Pure Appl. Chem.* **1992**, *64*, 1319.
- (17) Harriman, A.; Heitz, V.; Sauvage, J.-P. *J. Phys. Chem.* **1993**, *97*, 5940.
- (18) Steenken, S. *Free Radical Res. Commun.* **1992**, *16*, 349.
- (19) Steenken, S.; Telo, J. P.; Novais, H. M.; Candais, L. P. *J. Am. Chem. Soc.* **1992**, *114*, 4701.
- (20) Kittler, L.; Lober, G.; Gollmick, F.; Berg, H. *J. Electroanal. Chem.* **1980**, *116*, 503.
- (21) Shafirovich, V. Y.; Courtney, S. H.; Ya, N.; Geacintov, N. E. *J. Am. Chem. Soc.* **1995**, *117*, 4920.
- (22) Mann, J. S.; Shibata, Y.; Meehan, T. *Bioconjugate Chem* **1992**, *3*, 554.
- (23) Telser, J.; Cruickshank, K. A.; Morrison, L. E.; Netzel, T. L. *J. Am. Chem. Soc.* **1989**, *111*, 6966.
- (24) Yamana, K.; Letsinger, R. L. *Nucleic Acids Symp. Ser.* **1985**, *16*, 169.
- (25) Yamana, K.; Gokota, T.; Ozaki, H.; Nakano, H.; Sengen, O.; Shimidzu, T. *Nucleosides Nucleotides* **1992**, *11*, 383.
- (26) Manoharan, M. In *Antisense Research and Applications*; Crooke, S. T., Lebleu, D., Eds.; CRC Press: Boca Raton, FL, 1993; p 303.
- (27) Yamana, K.; Nunota, K.; Nakano, H.; Sengen, O. *Tetrahedron Lett.* **1994**, *35*, 2555.
- (28) Koenig, P.; Reines, S. A.; Cantor, C. R. *Biopolymers* **1977**, *16*, 2231.
- (29) Kierzek, R.; Li, Y.; Turner, D. H.; Bevilacqua, P. C. *J. Am. Chem. Soc.* **1993**, *115*, 4985.
- (30) Eriksson, M.; Kim, S. K.; Sen, S.; Graslund, A.; Jernstrom, B.; Norden, B. *J. Am. Chem. Soc.* **1993**, *115*, 1639.
- (31) Kim, S. K.; Geacintov, N. E.; Zinger, D.; Sutherland, J. C. In *Brookhaven Symposium in Biology, No. 35. Synchrotron Radiation in Biology*; Brookhaven National Laboratory: Upton, NY, 1988.
- (32) Slama-Schwok, A.; Jazwinski, J.; Bere, A.; Montenay-Garestier, T.; Rougee, M.; Helene, C.; Lehn, J.-M. *Biochemistry* **1989**, *28*, 3227.
- (33) Kubota, T.; Kano, J.; Uno, B.; Konse, T. *Bull. Chem. Soc. Jpn.* **1987**, *60*, 3865.
- (34) Zana, R.; Lang, J.; Lianos, P. *Polym. Prepr.* **1982**, *23*, 39.
- (35) Lianos, P.; Dupontail, G. *Eur. Biophys. J.* **1992**, *21*, 29.
- (36) Lianos, P. *Natō Asi Ser., Ser. C* **1990**, *324*, 309.
- (37) Dupontail, G.; Brochon, J. C.; Lianos, P. *J. Phys. Chem.* **1992**, *96*, 1460.

- (38) Argyrakis, P.; Duportail, G.; Lianos, P. *J. Chem. Phys.* **1991**, *95*, 3808.
- (39) Yamana, K.; Ohashi, Y.; Nunota, K.; Kitamura, M.; Makano, H.; Sangan, O.; Shimidzu, T. *Tetrahedron Lett.* **1991**, *32*, 6347.
- (40) Bevilacqua, P. C.; Kierzek, R.; Johnson, K. A.; Turner, D. H. *Science (Washington D.C.)* **1992**, *258*, 1355.
- (41) Breslauer, K. J.; Frank, R.; Blocker, R.; Marky, L. A. *Proc. Natl. Acad. Sci. U.S.A.* **1986**, *83*, 3746.
- (42) Marky, L. A.; Breslauer, K. J. *Biopolymers* **1987**, *26*, 1601.
- (43) Meade, T. J.; Kayyem, J. F. *Angew. Chem., Int. Ed. Engl.* **1995**, *34*, 352.
- (44) Lecomte, J. P.; Kirsch-De Mesmaeker, A.; Kelly, J. M.; Tossi, A. B.; Goerner, H. *Photochem. Photobiol.* **1992**, *55*, 681.
- (45) Brun, A. M.; Harriman, A. *J. Am. Chem. Soc.* **1992**, *114*, 3656.
- (46) Janovic, S. V.; Simic, M. *Biochim. Biophys. Acta* **1989**, *1008*, 39.
- (47) Cullis, P. M.; Jones, G. D. D.; Symons, M. C. R.; Lea, J. S. *Nature* **1987**, *330*, 773.
- (48) Brun, A. M.; Harriman, A. *J. Am. Chem. Soc.* **1991**, *113*, 8153.
- (49) Candeias, L. P.; Wolf, P.; O'Neill, P.; Steenken, S. *J. Phys. Chem.* **1992**, *96*, 10302.
- (50) Turro, N. J.; Barton, J. K.; Tomalia, D. In *Photochem. Convers. Storage Sol. Energy, Proc. Int. Conf., 8th, Meeting Date 1990*; Pelizzetti, E., Schiavello, M., Eds.; Kluwer: Dordrecht, The Netherlands, 1991; p 121.
- (51) Rissler, S. M.; Beratan, D. N.; Meade, T. J. *J. Am. Chem. Soc.* **1993**, *115*, 2508.
- (52) Sessler, J. L.; Capuano, V. L.; Harriman, A. *J. Am. Chem. Soc.* **1993**, *115*, 4618.
- (53) Murphy, C. J.; Arkin, M. R.; Jenkins, Y.; Ghatlia, N. D.; Bossmann, S. H.; Turro, N. J.; Barton, J. K. *Science* **1993**, *262*, 1025.
- (54) Candeis, L. P. *Radiation chemistry of purines in aqueous solution*; Inst. Super. Tec., Tech. Univ. Lisbon, Lisbon, Port.: Report Order No. PB92-229418, 174 pp; (Port.) Avail. NTIS From Gov. Rep. Announce. Index (U.S.) 1992, 92(23), Abstr. No. 265,515., 1992.
- (55) Michalik, V. *Int. J. Radiat. Biol.* **1992**, *62*, 9.
- (56) Sevilla, M. D. *Mechanisms for Radiation Damage in DNA. Comprehensive Report, June 1, 1986-May 31, 1992*; U.S. Department of Energy, Division of Energy Research: INIS 23:29887 DOE/ER/60455-6, 1991.
- (57) Schulte-Frohlinde, D.; Von, S. C. *UCLA Symp. Mol. Cell. Biol., New Ser.* **1990**, *136*, 31.
- (58) Bien, M.; Steffen, H.; Schulte-Frohlinde, D. *Mutat. Res.* **1988**, *194*, 193.
- (59) Schulte-Frohlinde, D.; Bothe, E. *NATO ASI Ser., Ser. H* **1991**, *54*, 317.
- (60) Manoharan, M.; Tivel, K. L.; Andrade, L. K.; Cook, P. D. *Tetrahedron Lett.*, in press.
- (61) Wagner, D.; Verheyden, J. P. H.; Moffat, J. G. *J. Org. Chem.* **1974**, *39*, 24.
- (62) Manoharan, M.; Tivel, K. L.; Cook, P. D. *Tetrahedron Lett.*, submitted.
- (63) Landon, T., private communication, Molecular Probes, Inc., 1994.
- (64) Fasman, G. D., Ed. *Handbook of Biochemistry and Molecular Biology: Nucleic Acids*; CRC Press: Cleveland, OH, 1975; Vol. 1, p 589.
- (65) Berlman, I. B. *Handbook of Fluorescence Spectra of Aromatic Molecules*; Academic Press: New York, 1971.
- (66) Lakowicz, J. R. *Principles of Fluorescence Spectroscopy*; Plenum Press: New York, 1986.
- (67) Weber, G.; Teale, F. W. *Trans. Faraday Soc.* **1957**, *53*, 646.
- (68) Parker, C. A.; Rees, W. T. *Analyst (London)* **1960**, *85*, 587.
- (69) Parker, C. A. *Photoluminescence of Solutions. With Applications to Photochemistry and Analytical Chemistry*; Elsevier: Amsterdam, 1968.
- (70) Demas, J. N.; Crosby, G. A. *J. Phys. Chem.* **1971**, *75*, 991.
- (71) Vix, A.; Lami, H. *Biophys. J.* **1995**, *68*, 1145.
- (72) Rehm, D.; Weller, A. *Isr. J. Chem.* **1970**, *8*, 259.
- (73) Brunschwig, B. S.; Ehrenson, S.; Sutin, N. *J. Phys. Chem.* **1986**, *90*, 3657.
- (74) Sutin, N.; Brunschwig, B. S.; Creutz, C.; Winkler, J. R. *Pure Appl. Chem.* **1988**, *60*, 1817.
- (75) Marcus, R. A.; Sutin, N. *Biochim. Biophys. Acta* **1985**, *811*, 265.
- (76) Geacintov, N. E.; Mao, B.; France, L. L.; Zhao, R.; Chen, J.; Liu, T. M.; Ya, N. Q.; Margulis, L. A.; Sutherland, J. C. *Proc. SPIE Int. Soc. Opt. Eng.* **1992**, *1640*, 774.
- (77) Faraggi, M.; Klapper, M. H. *J. Chim. Phys.* **1994**, *91*, 1054.
- (78) Faraggi, M.; Klapper, M. H. *J. Chim. Phys.* **1994**, *91*, 1062.
- (79) Wang, W.; Sevilla, M. D. *Radiat. Res.* **1994**, *138*, 9.
- (80) Cullis, P. M.; McClymont, J. D.; Malone, M. E.; Mather, A. N.; Podmore, I. D.; Sweeney, M. C.; Symons, M. C. R. *J. Chem. Soc., Perkin Trans. 2* **1992**, 695.
- (81) Barnes, J.; Bernhard, W. Q. *J. Phys. Chem.* **1993**, *97*, 3401.
- (82) Barnes, J. P.; Bernhard, W. A. *J. Phys. Chem.* **1994**, *98*, 887.
- (83) Perichon, J. In *Encyclopedia of Electrochemistry of the Elements, Organic Section*; Bard, A. J., Lund, H., Eds.; Marcel Dekker, Inc.: New York, 1978; Vol. 11, p 108.
- (84) Pysh, E. S.; Yang, N. G. *J. Am. Chem. Soc.* **1963**, *85*, 2124.
- (85) Gough, T. A.; Peover, M. E. *Polarography 1964*; **1964**, 1017.
- (86) Bolton, J. R.; Archer, M. D. In *Electron Transfer in Inorganic, Organic, and Biological Systems*; Bolton, J. R., Mataga, N., McLendon, G., Eds.; American Chemical Society: Washington, D.C., 1991; p 7.
- (87) Brunschwig, B. S.; Ehrenson, S.; Sutin, N. *J. Phys. Chem.* **1987**, *91*, 4714.
- (88) Closs, G. L.; Miller, J. R. *Science (Washington D.C.)* **1988**, *240*, 440.
- (89) DeVault, D. *Q. Rev. Biophys.* **1980**, *13*, 387.
- (90) Dutton, P. L. *Electron transfer mechanisms in reaction centers: final progress report*; DOE/ER/13476-1: Avail. NTIS From: Energy Res. Abstr. 1989, 14(24), Abstr. No. 52056 DE90001204, 1989.
- (91) Gray, H. B.; Winkler, J. R. *Pure Appl. Chem.* **1992**, *64*, 1257.
- (92) Marcus, R. A. *Chem. Phys. Lett.* **1988**, *133*, 471.
- (93) Paddon-Row, M. N.; Oliver, A. M.; Warman, J. M.; Smit, K. J.; De Haas, M. P.; Oevering, H.; Verhoeven, J. W. *J. Phys. Chem.* **1988**, *92*, 6958.
- (94) Ho, P. S. *DNA-mediated Electron Transfer and Application to 'Biochip' Development*; Gov. Rep. Announce. Index (U. S.) 1991, 91(23), Abstr. No. 165,497: Report, Order No. AD-A239093, 6 pp. Avail. NTIS, 1991.
- (95) Brun, A. M.; Harriman, A. *NATO ASI Ser., Ser. C* **1992**, *371*, 395.
- (96) Nese, C.; Yuan, Z.; Schuchmann, M. N.; Von Sonntag, C. *Int. J. Radiat. Biol.* **1992**, *62*, 527.
- (97) Lin, N. *Res. Chem. Intermed.* **1990**, *14*, 209.
- (98) Turro, C.; Chang, C. K.; Leroi, G. E.; Cukier, R. I.; Nocera, D. G. *J. Am. Chem. Soc.* **1992**, *114*, 4013.
- (99) Kitzinger, A.; Port, H. *Chem. Phys. Lett.* **1991**, *184*, 11.
- (100) Kano, K.; Matsumoto, H.; Hashimoto, S.; Sisido, M.; Imanishi, Y. *J. Am. Chem. Soc.* **1985**, *107*, 6117.
- (101) Inai, Y.; Sisido, M.; Imanishi, Y. *J. Phys. Chem.* **1990**, *94*, 8365.
- (102) Koshioka, M.; Misawa, H.; Sasaki, K.; Kitamura, N.; Masuhara, H. *J. Phys. Chem.* **1992**, *96*, 2909.
- (103) Duhamel, J.; Winnik, M. A.; Baros, F.; Andre, J. C.; Martinho, J. M. G. *J. Phys. Chem.* **1992**, *96*, 9805.
- (104) Lianos, P.; Zana, R. *J. Phys. Chem.* **1980**, *84*, 3339.
- (105) Lianos, P.; Georghiou, S. *Photochem. Photobiol.* **1979**, *29*, 13.
- (106) Brahmans, J.; Brahmans, S. In *Fine Structure of Proteins and Nucleic Acids*; Fasman, G. D., Timasheff, S. N., Eds.; Marcell Dekker, Inc.: New York, 1970; Vol. 4, p 191.
- (107) Johnson, C. W. In *Circular Dichroism: Interpretation and Applications*; Nakarishi, K., Berova, N., Woody, R. W., Eds.; VCH Publishers: New York, 1994; p 523.
- (108) Zehfus, M. H.; Johnson, W. C. *J. Biopolymers* **1981**, *20*, 1589.
- (109) Zehfus, M. H.; Johnson, W. C. *J. Biopolymers* **1984**, *23*, 1269.
- (110) Graslund, A.; Kim, S. K.; Eriksson, S.; Norden, B.; Jernstroem, B. *Biophys. Chem.* **1992**, *44*, 21.
- (111) van Houte, L. P. A.; van Grondelle, R.; Retel, J.; Westra, J. G.; Zinger, D.; Sutherland, J. C.; Kim, S. K.; Geacintov, N. E. *Photochem. Photobiol.* **1989**, *49*, 387.